Toward Understanding and Optimizing the Template-Guided Synthesis of Chiral Polyaniline Nanocomposites

Wenguang Li,[†] Patrick A. McCarthy,[†] Dingguo Liu,[†] Jianyu Huang,[‡] Sze-Cheng Yang,[§] and Hsing-Lin Wang*,[†]

Bioscience Division, MSJ586, Los Alamos National Laboratory, Los Alamos, New Mexico 87545; Materials Science Division, Los Alamos National Laboratory, Los Alamos, New Mexico 87545; and Chemistry Department, University of Rhode Island, Kingston, Rhode Island 02881

Received June 12, 2002; Revised Manuscript Received October 21, 2002

ABSTRACT: Previously we reported synthesis and characterization of water-soluble chiral conducting polymer nanocomposites via template-guided synthesis. Experimental procedures and parameters need to be carefully controlled to achieve synthesis of water-soluble nanocomposites. Here, we describe a modified synthetic procedure with higher molecular weight poly(acrylic acid) (PAA) (MW ∼ 250 000) as a template. This new system allows synthesis of chiral water-soluble nanocomposites over a more broad range of conditions making the synthesis more reproducible and easier to carry out at large scale. Another objective of this work is to further understand the underlying formation mechanism of chiral polyaniline nanocomposites. We carried out a detailed study of how temperature, template, and solvent affect the final morphology and properties of these nanocomposites. We found that the extent of interaction and stability of the template/monomer/acid adduct (nanocomposite precursor) and population density of monomer surrounding the template are crucial in determining the degree of nanocomposite chirality. Detailed characterization of the nanocomposites and their precursors was carried out by circular dichroism (CD), UV−vis, FTIR, NMR, and TEM spectroscopy. On the basis of experimental results and synthetic procedures, a simplified model for the formation mechanism of chiral polyaniline nanocomposite is proposed.

Introduction

Conducting polymer (organic/inorganic) nanocomposites were first synthesized by polymerizing monomers such as pyrrole, aniline, and thiophene in the presence of various metal oxides.[1−3] Water-soluble polymers and polyelectrolytes have been used as steric stabilizers for the synthesis of nanocomposites containing conducting polymers (organic/organic).[4−9] Organic/organic nanocomposites containing conducting polymers have also been synthesized by template-guided synthesis.[4−9] These nanocomposites have been referred to as colloids or dispersions depending on their morphology and water solubility. Nanocomposites have novel charge storage,[10,11] magnetic,[12] and catalytic properties[13] and have potential applications in fabricating optoelectronic devices. Recently, chiral conducting polymer nanocomposites were synthesized electrochemically[14,15] and chemically[16] by polymerizing monomers in the presence of both water-soluble polymers and optically active acids. Optically active conducting polymer nanocomposites are of particular importance to the development of polymer-based chemical separation materials. They possess both the optical and electronic properties and have potential applications as surface-modified electrodes,[17,18] stationary phases for chiral separations,[19] and sensors for detecting the presence of chiral molecules. Chiral polyaniline (PANI),[20−22] polypyrrole,[23] and polyacetylene,[24] polythiophene,[25] and poly(phenylenevinylene)[25] have all been synthesized. Chirality from the conjugated backbone of conducting polymers is believed to be due to helical conformation of main chains.[26] In addition, the helical conjugated polymer was prepared by interaction between achiral conjugated polymer and with small chiral molecules via acid−base interaction.[27] Synthesis of helical (optical active) conjugated polymers is typically carried out by either polymerizing chiral monomers or simply introducing small chiral molecules into the polymer solution knowing that they will interact with the achiral polymer to form a helical conformation.[21,27] For most applications, it is crucial to have chiral polymers that are water-soluble or dispersible so that they can be processed. Therefore, our goal is to achieve a greater understanding of the underlying formation mechanism and optimize the synthesis of chiral, water-soluble polyaniline nanocomposites.

Previously, we reported the template-guided synthesis of water-soluble chiral nanocomposites using a chiral camphorsulfonic acid (CSA) as chiral inducing agent and poly(acrylic acid) (90 000 MW) as a template.[16] These chiral nanocomposites are very stable, and they can be made into large quantities. The chirality of PAA/PANI/CSA was induced by the chiral dopant, CSA, and the chirality remained after we replace the chiral acid with HCl. We believe the template (PAA) stabilizes the polyaniline chiral conformation, therefore no longer requiring the presence of the chiral acid to maintain its optical activity. We have suggested this template-guided synthesis is first forming a complex between aniline (AN), PAA, and CSA. Although it has been established that CSA helps to generate chiral PANI during aniline polymerization, the mechanism and reaction conditions that control chiral PANI formation are still lacking.

In this paper, we carried out template-guided polymerization of chiral PAA/PANI nanocomposites using a simplified procedure based on high molecular weight poly(acrylic acid) (250 000 MW). This new procedure allows us to synthesize water-soluble nanocomposites in a more broad concentration range. To further under-

[†] Bioscience Division, MSJ586, Los Alamos National Laboratory.
[‡] Materials Science Division, Los Alamos National Laboratory.
[§] University of Rhode Island.
* Corresponding author: e-mail hwang@lanl.gov.

10.1021/ma020915t CCC: $22.00
Published on Web 12/07/2002

Table 1. Addition Sequence of Doping/Dedoping Cycles[a]

	test tube no.						
	1	2	3	4	5	6	7
1st addition	NaCl	NaOH	NaOH	NaOH	NaOH	NaOH	NaOH
2rd addition	NaCl	NaCl	HCl	HCl	HCl	HCl	HCl
3th addition	NaCl	NaCl	NaCl	NaOH	NaOH	NaOH	NaOH
4th addition	NaCl	NaCl	NaCl	NaCl	HCl	HCl	HCl
5th addition	NaCl	NaCl	NaCl	NaCl	NaCl	NaOH	NaOH
6th addition	NaCl	NaCl	NaCl	NaCl	NaCl	NaCl	HCl
final solution	A1	B1	A2	B2	A3	B3	A4

[a] NaOH = 20 μL of 0.1 M NaOH solution, HCl = 20 μL of 0.1 M HCl, NaCl = 20 μL of 0.05 M NaCl.

stand the underlying formation mechanism of chiral nanocomposites, we studied the PAA/PANI/CSA nanocomposite precursor (PAA/AN/CSA) and the relationship between chirality and synthesis conditions such as total concentration, ratio of PAA to AN, solvents, and temperature. On the basis of our experimental results, we speculate toward a mechanism for chiral formation within PAA/PANI nanocomposites.

Experimental Section

Instrument and Materials. Aniline, (1*S*)-(+)-10-camphorsulfonic acid, poly(acrylic acid) (250 000 MW), poly(vinyl methy ether-*alt*-maleic acid), PMVEMA, and ammonium persulfate were purchased from Aldrich and were used as received. Ultrapure water (resistivity, >18 MΩ/cm) was used in all polymer nanocomposite solutions and in all membrane dialysis. Dialysis of polyaniline nanocomposite solution was carried out by using a Spectra/Por membrane with molecular weight cutoff at ~3500 Da.

Chiral polyaniline nanocomposites and their precursor were characterized by UV−vis, CD, FTIR, NMR, and TEM spectroscopy. Circular dichlorism spectra (CD) were taken using a Jasco 710 spectrometer, and the scan rate was 100 nm/min. The spectra obtained were the average of three scans. The CD samples were prepared by diluting PANI nanocomposites to 0.7 mM, calculated based on the initial amount of AN monomer used and 100% conversion rate, and an aliquot was transferred to a 2 mm quartz cell. UV−vis spectra were measured by a Perkin-Elmer Lamda 19 spectrometer using the same quarts cell as CD measurement. The FTIR samples were prepared by droping diluted nanocomposite solutions on top of a AgF substrate, and the spectra were obtained on a Nicolet Magna-IR 750 spectrometer. NMR spectra were measured in D_2O with the 500 MHz Bruker drx 500 spectrometer. Transmission electron micrographs were taken by a Philips CM-30 transmission electron microscope.

Synthesis of Polyaniline Nanocomposites. In a typical procedure, 0.3 g of PAA(4.17 mmol, per repeat unit), 0.2 g of aniline (2.15 mmol), and 0.75 g of CSA (3.23 mmol) were codissolved in 10 mL of deionized water. The solution mixture was stirred for 24 h. Then a 5 mL aqueous solution containing 0.49 g of ammonium persulfate (2.15 mmol) was added. Dark-green water-soluble PAA/PANI/CSA nanocomposite was obtained in a few hours. Spectra/Pro dialysis membrane with molecular weight cutoff at 3500 Da was used to purify the dispersible products.

Doping/Dedoping Cycles of Chiral Complexes. A purified chiral PAA/PANI/HCl nanocomposite solution was diluted with deionized water to 3.5 mM. 1 mL of the diluted solution was added to seven different test tubes marked from one to seven. The doping and dedoping cycles were accomplished by adding 20 μL of 0.1 M NaOH and 20 μL of 0.1 M HCl to all seven test tubes in a sequence (see Table 1). UV−vis and CD spectra were taken after all the additions were accomplished. Based on this procedure, all seven solutions had the same volume, concentration, and salt content. This is because after each doping and doping cycle 40 μL of 0.05 M NaCl was generated due to reaction between NaOH and HCl. The same amount of NaCl solution was added to the other test tubes to balance the salt and volume changes. Between each addition, the solutions were allowed to equilibrate while stirring for 1 h. 0.1 mL of the final solution was added to a 2 mm quartz cell and diluted to 0.5 mL before UV−vis and CD measurements were taken. The final PANI nanocomposite concentration is estimated to be 0.7 mM. The number of moles of PANI is calculated by assuming the full conversion of AN monomers to PANI and using its tetramer repeat unit as the PANI molecular weight. The molecular structures of the doped and dedoped PANI (tetramer repeat unit) are shown in Scheme 1. Since the nanocomposites are composed of both PANI and PAA, we use the concentration of PANI to represent the concentration of PANI nanocomposite.

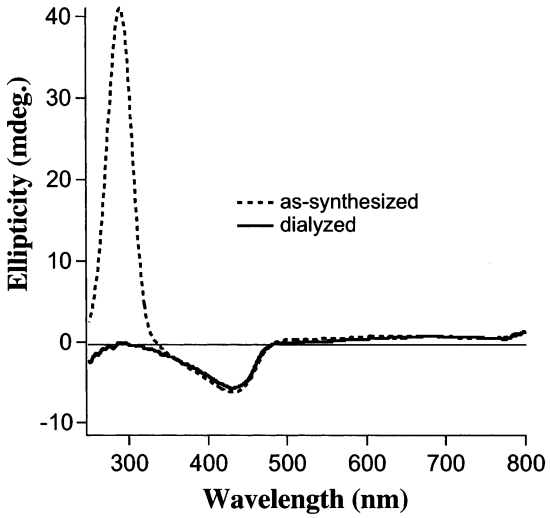

Figure 1. CD spectra of the as-synthesized and dialyzed PANI nanocomposites.

Scheme 1. Molecular Structures of the Tetrameric Repeat Unit of Doped and Dedoped Polyaniline

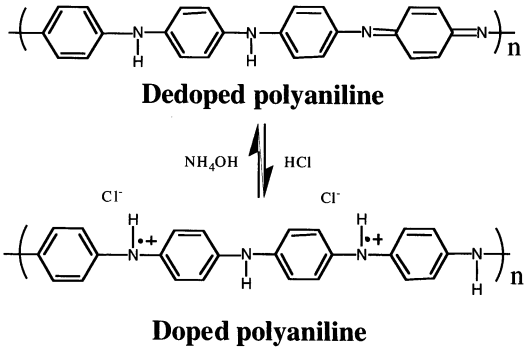

Results and Discussion

The as-synthesized PAA/PANI/(+)-CSA nanocomposite dispersed nicely in aqueous solution, and the CD spectra are shown in Figure 1. There are three peaks; the peak at 290 nm is due to (+)-CSA and the other two peaks resulting from chiral polyaniline, one strong negative peak at 440 nm and a broad peak extending

Scheme 2. Simplified Schematic Representation of Template-Guided Synthesis Based on Water-Soluble Polymer

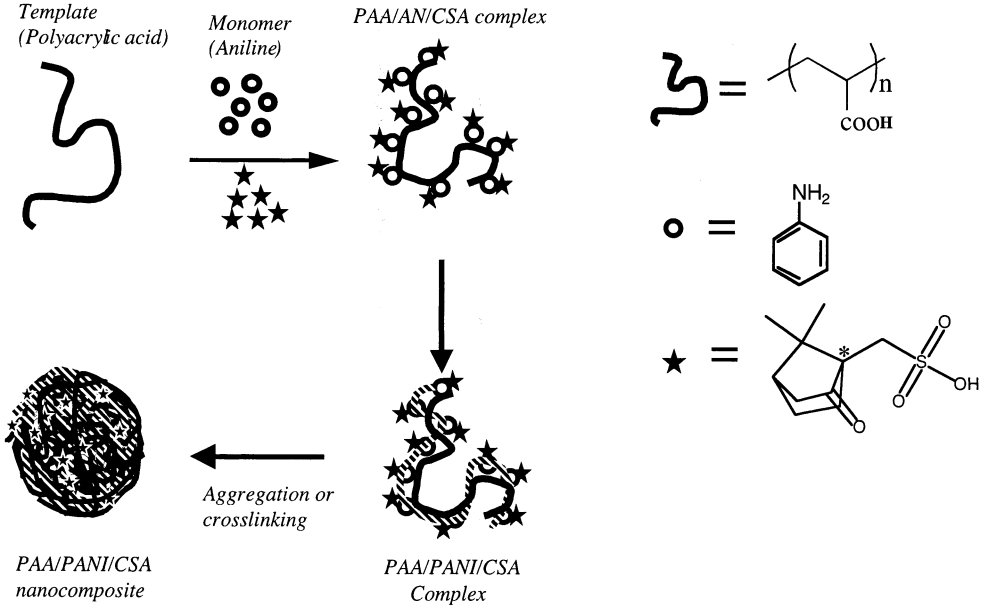

from 500 to 800 nm. These two CD peaks are associated with the PANI UV−vis absorption at 400 and around 800 nm, respectively. The as-synthesized PAA/PANI/CSA nanocomposite was then purified by dialysis against HCl. After dialysis, (+)-CSA was removed, and the CD peak at 290 nm is no longer observed; however, CD peaks from PANI remain. Both the CD intensity and UV−vis absorption due to PANI decrease slightly. This can be explained by the decrease of nanocomposite concentration resulting from diffusion of water into the dialysis tube driven by the concentration difference on both sides of the tube. This result suggests that the chiral signal is indeed resulting from chiral polyaniline. Since there is no chiral centers in either PAA or PANI, chirality of PAA−PANI is induced by optically active CSA. Once the polymer's chiral conformation is formed, it no longer requires CSA to maintain its chirality.

A TEM micrograph of the as-synthesized nanocomposites is shown in Figure 2. In this figure we observe inhomogeneity of nanocomposite morphology and a relatively large size distribution where nanocomposite length ranges from 50 to 300 nm and nanocomposite width ranges from 30 to 100 nm. Electron diffraction of the reaction product indicates that the nanocomposites is completely amorphous (figure not shown). Our previous study found PAA/PANI nanocomposites to have a narrow size distribution.[28] The reason for this discrepancy may be twofold. First, 90 000MW PAA was used in the previous study, and 250 000MW PAA was used in this study. Second, the template-guided synthesis was carried out with a slightly modified procedure. In this study AN/CSA was added to a solution containing PAA and stirred for 24 h. In the previous paper, AN was added to a solution containing PAA and stirred 24 h; then, CSA was added just before polymerization. For both systems, our hypothesis involves optically active CSA complexing with aniline through acid−base interaction. This complex can be considered as chiral aniline (monomer). The chiral monomers surrounding the PAA template give rise to a locally higher aniline concentration. Polymerizing AN/CSA may lead to chiral PANI. In this paper, we propose a simplified step-by-step reaction mechanism and design experiments to further elucidate the formation mechanism of the chiral nanocomposites (Scheme 2).

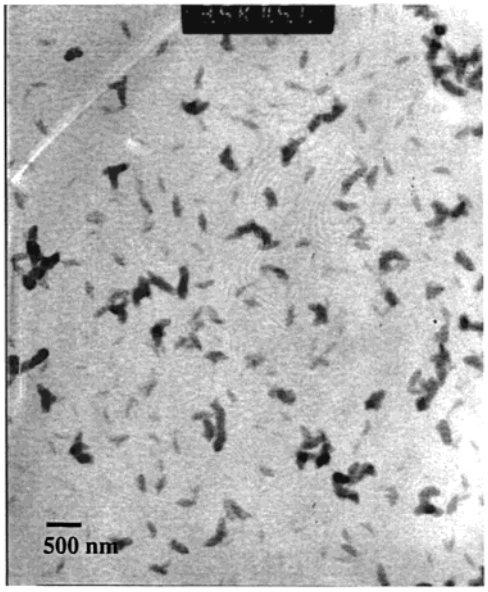

Figure 2. TEM micrograph of PAA/PANI/CSA nanocomposites.

1. Effect of Overall Concentration. The overall solution concentration has a significant impact in the chirality of PAA/PANI/CSA nanocomposites. In this experiment, we kept the amount of PAA, AN, and CSA constant and the molar ratio (PAA:AN:CSA = 2:1:1.5) constant. We vary the overall concentration by adding different amounts of total solvent (water) from 10 to 120 mL. In all cases, we obtained products that were water-dispersible, which demonstrates that this synthesis can be carried out over a much greater concentration range than the previous study.[28] PANI nanocomposite solutions from these reactions were diluted to 0.7 mM before CD spectra were measured. UV−vis of the absorbance intensity of these solutions was also measured to ensure the same amount of nanocomposite was used for each measurement. The CD spectra of these PANI nanocomposites are shown in Figure 3. The CD intensity of PANI nanocomposite decreases as the total concentration prior

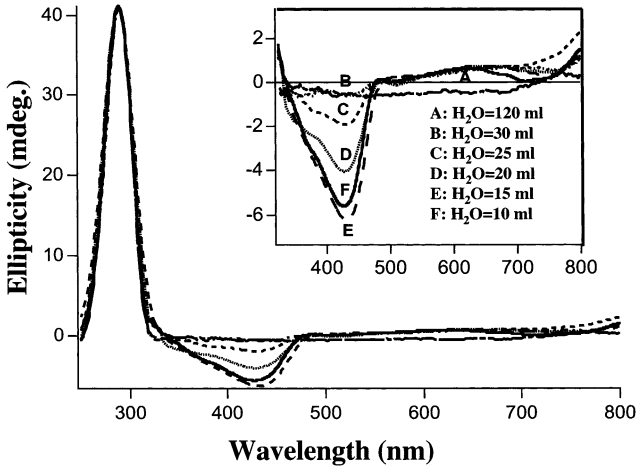

Figure 3. CD spectra of the as-synthesized PANI nanocomposites synthesized under different concentrations.

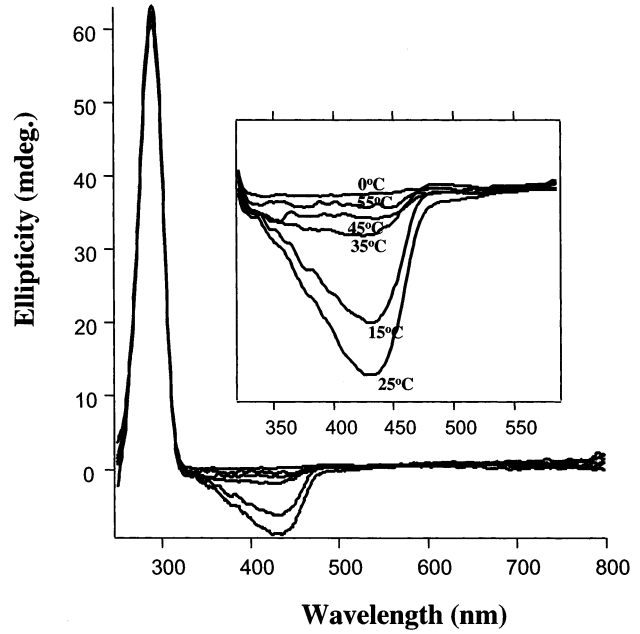

Figure 4. Effect of temperature on the chirality of PAA/PANI/CSA nanocomposites.

to synthesis decreases. PANI CD peaks became almost invisible when the water added exceeded 30 mL. Note that the final solution color remains dark green with water medium exceeding 30 mL. There seems to be a threshold concentration in order to form chiral polyaniline nanocomposites. Below this critical concentration, chiral PAA/PANI cannot be synthesized. The optimum synthetic condition found is when the molar ratio of PAA:AN:CSA is fixed at 2:1:1.5, and the concentration of PAA is around 1% and 2% CSA which gave the highest CD signals. Higher concentration beyond the optimum condition results in slight decreases in the chirality. This result suggests the importance of the overall concentration and the stability of the PAA/AN/CSA complex that leads to chiral nanocomposites after polymerization.

2. Effect of Solvents. Another way to fine-tune the interactions among monomer, template, and chiral acid is through changing the dielectric of the reaction media. Although there is no problem dissolving the nanocomposite precursor (PAA/AN/CSA complex) in solvents such as ethanol, propanol, and acetone, the oxidant, ammonium persulfate, is not soluble in any of the above solvents. Therefore, we use a mixed solvent system, which contains 50% water and 50% ethanol, 2-propanol, acetic acid, or acetone. The rest of the experimental parameters are kept constant as described previously

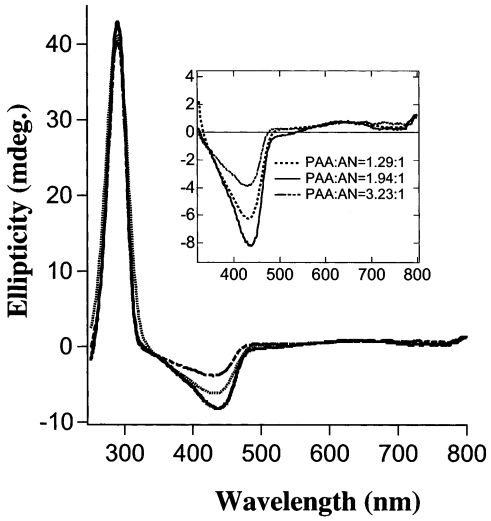

Figure 5. Effect of PAA:AN molar ratio on the chirality of the PAA/PANI/CSA nanocomposites.

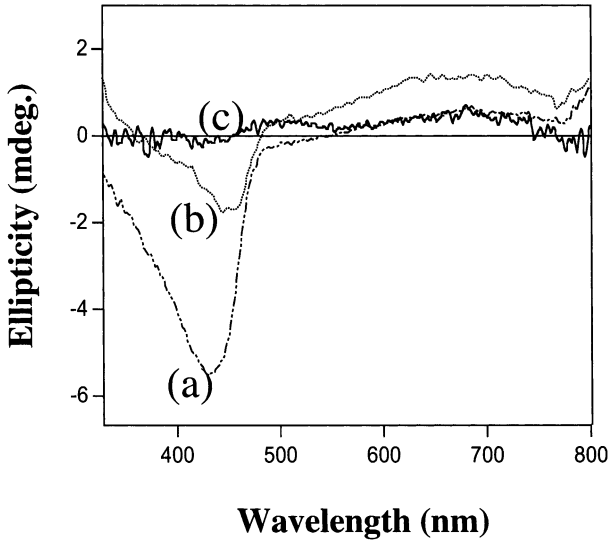

Figure 6. Effect of template on the chirality of the as-synthesized nanocomposites (a) PAA, (b) PVMEMA, and (c) no template.

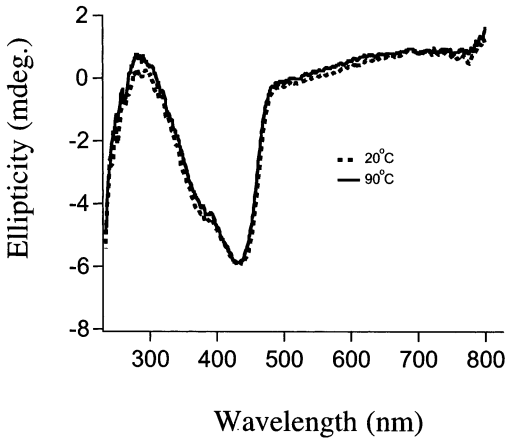

Figure 7. CD spectra of PAA/PANI/CSA nanocomposite at temperature of 20 and 90 °C.

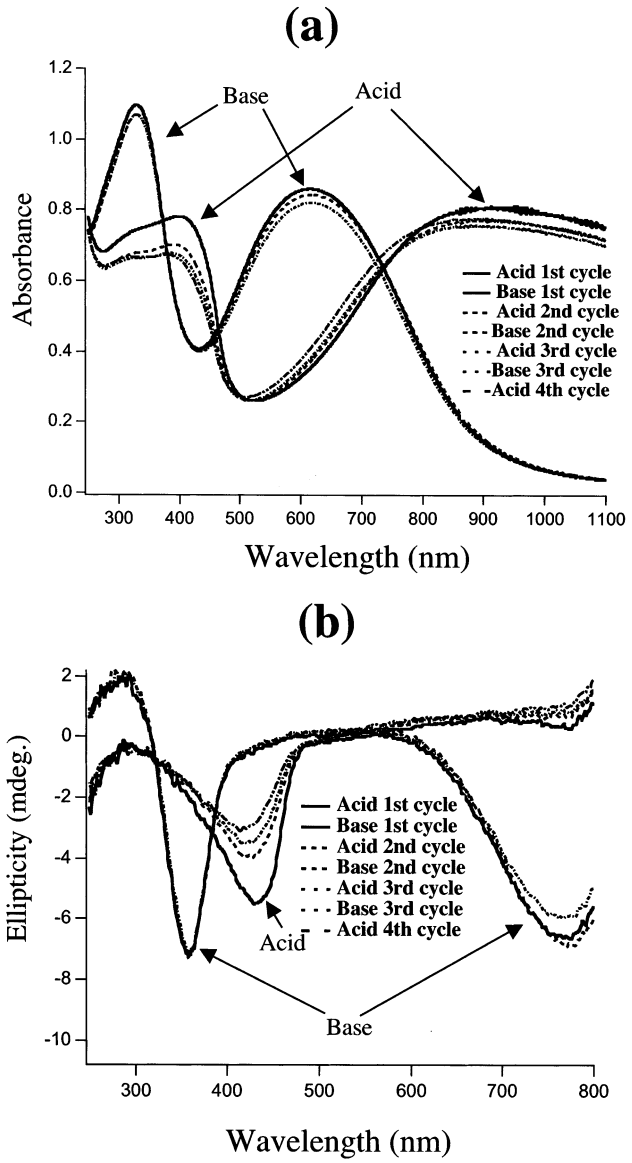

Figure 8. UV−vis (a) and CD (b) spectra of PANI chiral nanocomposite under repeated doping and dedoping cycles.

in the Experimental Section. The final products from the mixed solvent systems were viscous solutions and gave very weak CD signals. These results support that the interaction between aniline and CSA (acid−base interaction) plays an important role in the formation of chiral PANI complexes. This acid−base interaction is expected to be weaker in the presence of organic solvents, which lower the dielectric constant of the reaction medium. This reduced acid−base interaction is thought to contribute to destabilization of the PAA/AN/CSA complex, thus reducing nanocomposite chirality.

3. Effect of Temperature. High molecular weight polyaniline is typically synthesized at low temperatures because low temperatures favor propagation over competitive side reactions.[29,30] We expect a similar effect in the synthesis of chiral nanocomposites. We also hoped that minimizing the side reactions would not only provide high molecular weight PANI but would also give high chirality because lower temperatures may stabilize the polyaniline nanocomposite precursor. CD spectra of six separate nanocomposites syntheses carried out at temperatures ranging from 0 to 55 °C are shown in Figure 4. To our surprise, the highest chirality of poly-

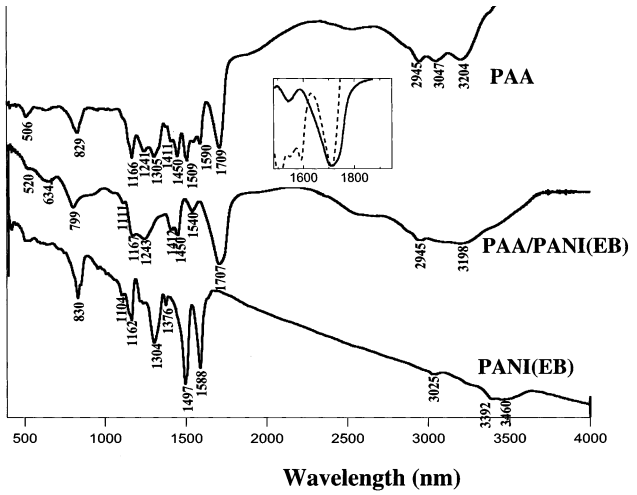

Figure 9. Infrared spectra of PANI (EB), PAA, and PAA/PANI nanocomposite. Inset shows the comparison of the carbonyl peaks between PAA (dash line) and PAA/PANI (solid line).

aniline nanocomposites is synthesized at 25 °C. Synthesis carried out at 0 °C gave only achiral products. Raising the temperature also gave nanocomposites with reduced chirality. Both high and low temperatures favor the formation of achiral product. We believe that higher temperatures destabilize the PAA/AN/CSA complex (see Scheme 2), increase dissociation of PAA/AN/CSA complex, and therefore result in achiral product. We believe that lower temperatures result in slow chain growth, allowing smaller sulfate ions from oxidant decomposition to compete with the optically active CSA before the chiral PANI is formed. Stability of the PAA/AN/CSA precursor appears to dominate nanocomposite chirality.

4. Effect of Molar Ratio between PAA and Aniline. Water-soluble PAA/PANI/CSA nanocomposites were synthesized with different PAA:AN molar ratios, and the CD spectra are shown in Figure 5. By increasing the molar ratio of PAA (monomer unit) to AN from 1.29:1 to 3.23:1, the intensity of the CD peak at 445 nm decreases from −8.5 to −3.5 mdeg. Since PANI UV/vis absorbances are the same for each solution, the difference in CD intensity is due to differences in the percentage of PANI existing in an optically active conformation. Because the nanocomposite chirality originated from polymerizing chiral monomers (AN/CSA) to form chiral polymer through asymmetric arrangement of aniline unites, densely populated chiral monomers surrounding the template results in nanocomposites with enhanced chirality. When the ratio of PAA to AN is high, the distance between chiral monomers surrounding the PAA is large, which in turn leads to nanocomposite with less chirality. If the ratio of PAA to aniline drops lower than 1:1, products precipitate. This result suggests that this reaction is not a homogeneous polymerization reaction that took place throughout the solution. Most of the aniline monomers stay somewhere near the templates. Although the overall aniline concentration is the same for all solutions, the local aniline concentration (near the template) depends on the concentration of the template.

5. Effect of Template. To further exam the effect of template on the chirality of nanocomposites, we use poly(vinyl methy ether-*alt*-maleic acid), PMVEMA, as a template. Since the template plays an important role in chiral PANI formation, we expect that the nature of

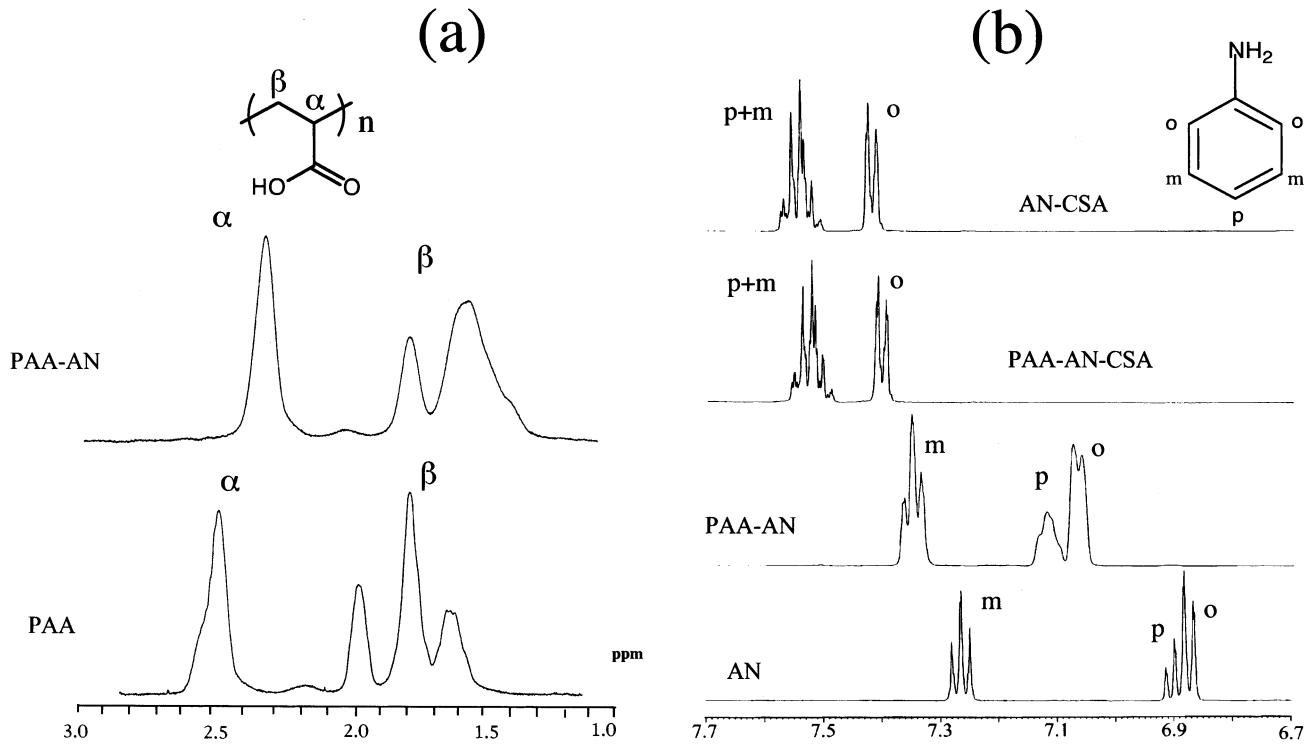

Figure 10. ^{1}H NMR spectra of (a) PAA, PAA/AN and (b) AN, PAA/AN, PAA/AN/CSA and AN/CSA.

the template would also influence chiral PANI formation. PMVEMA/PANI/CSA synthesis results in nanocomposite with a relatively weak CD signals. CD signals of the doped PMVEMA/PANI are different from and weaker than CD signals of PAA/PANI/CSA nanocomposites (see Figure 6). This result suggests that the nature of the template affects the chirality of PANI nanocomposites

In addition, conventional synthesis of PANI/CSA as a thin film on a glass substrate was carried out according to the "1-dip" in-situ deposition method, in the absence of PAA (template).[31] We follow this procedure to synthesize chiral PANI/CSA, except that the molar ratio was set at AN:CSA = 1:1.5 and the CSA concentration is at 0.3 M (CSA concentration is at 1.0 M according to the literature procedure). In this experiment, we insert a glass substrate into a reaction beaker containing aniline monomer and CSA. After initiating the polymerization reaction with ammonium persulfate, a PANI/CSA thin film was deposited onto the glass substrate along with a powdery precipitate inside the beaker. In contrast to the earlier report,[31] the resulting thin film and precipitate both show no chirality (Figure 6c), presumably due to lower overall CSA concentration.

Adding PAA template to the above reaction results in formation of chiral PANI nanocomposites (see Figure 6a). If formation of a CSA/AN complex is the only important event in chiral PANI formation, then we expect the absence of PAA to have little effect on the degree of PANI chirality. The above results suggest that CSA has a much greater efficiency for generating optically active PANI in the presence of PAA, and the presence of PAA is required for chiral PANI formation under some conditions (see Scheme 2). This results also suggests that template serves to pull together AN/CSA monomers in the vicinity of the template and hence increase the local AN/CSA concentration, thereby giving rise to chiral polyaniline interpolymer complexes which leads to formation of nanocomposite.

Stability of Chiral PAA−PANI. In an earlier experiment, we showed that synthesis of chiral PANI/PAA nanocomposites at elevated temperature (above 25 °C) resulted in decreased PANI optical activity. Since DNA and protein lose their helicity by increasing temperature, we would expect PANI optical activity to also decrease when it is heated. In fact, the unraveling of chiral[32] or helical[33] polymer conformation at elevated temperature is commonly observed. To further examine the stability of our chiral nanocomposites, we carried out experiments to determine their thermal and chemical stability. We heated the aqueous chiral PANI nanocomposites solution up to 90 °C. The CD spectra of PANI nanocomposites at 20 and 90 °C were basically identical (see Figure 7). This result supports our belief that PAA acts as a polymeric scaffold for stabilization of PANI chirality.

The chiral nanocomposites were also tested for their chemical stability by repeatedly doping and dedoping with 0.1 M HCl and 0.1 M NH_4OH. Their properties were monitored by CD and UV−vis spectroscopy (see Figure 8). The doped PANI peak at 440 nm drops slightly after every cycle, while the intensity of another peak between 500 and 800 nm increases slightly. CD spectra of the dedoped nanocomposite peaks (350 and 770 nm) remained essentially the same through three doping cycles. Since there is no loss or gain of material during doping−dedoping cycles, UV−vis and CD spectra of the doped PANI nanocomposite show slight intensity changes, suggesting some kind of PANI conformational change. The exact cause why the CD spectrum of doped PANINC shows a decrease of CD intensity is not clearly understood. The above results, however, do suggest as-synthesized chiral nanocomoposites are robust against acid and base.

Characterization. *FTIR*. The FTIR spectrum of PAA/PANI features vibrational characteristics of both the PAA and PANI emeraldine base (EB) polymers (Figure 9). For example, the nanocomposite composed

of PAA and EB features a carbonyl stretching band at 1707 cm^{-1}, CH_2− bending at 1450 cm^{-1}, and C−O stretching bands coupled with O−H in-plane bending at 1411 and 1241 cm^{-1}; these bands are associated with, and only with, PAA.[34,35] Meanwhile, other bands at 1590 and 1509 cm^{-1} from the stretching of C═C of the aromatic ring, 1306 cm^{-1} from C−N stretching, and 1166 cm^{-1} from C−H bending are all associated with, and only with, polyaniline (EB).[36,37] When we compare the IR spectrum of the PAA/PANI(EB) nanocomposite with the pure PAA and PANI, we observe a shift of most IR peaks from 1 to 10 cm^{-1},which suggests changes of environment at the molecular level. Inspection of Figure 9 shows the carbonyl peak of pure PAA and PAA/PANI; the nanocomposite peaks clearly demonstrate a narrower peak indicative of reduced hydrogen-bond interactions between carboxylic acid groups. Presumably, polyaniline disrupts PAA intra- and intermolecular hydrogen bonding.

NMR Spectroscopy. The interactions between PAA, AN, and CSA were studied by H^1 NMR spectroscopy. Comparing the ^{1}H NMR spectrum of PAA/AN with PAA and aniline, we have observed that both α and β protons of PAA were upfield shifted, while protons at the ortho, para, and meta positions of the AN benzene ring were downfield shifted (see Figure 10). This result suggests that the interaction between AN and PAA causes deshielding of AN. Judging from the molecular structures of PAA and AN (see Figure 10), H-bonding and acid−base interactions may contribute to the downfield chemical shift of AN. Addition of CSA to the AN/PAA solution caused the aromatic protons to shift further downfield (e.g., protons at the ortho position shift from 7.06, 7.07 ppm to 7.39, 7.41 ppm). Furthermore, the ^{1}H NMR spectrum of AN/CSA was similar to the PAA/AN/CSA. This similarity suggests that within the PAA/AN/CSA complex AN is mainly protonated by CSA.

In addition, we observe broadening of aniline proton peaks at ortho and para positions in the PAA/AN solution (Figure 10). Similar broadening of aniline proton peaks was observed when aniline was complexed with sodium dodecybenzenesulfonate micelles.[38] The aniline proton peak broadening was attributed to the inhomogeneous nature of the medium caused by the presence of micelle, which served as a template, and the aniline was intercalated with this template.[38] In our case we use PAA polyelectrolyte as a template. A possible explanation for our peak broadening is that AN monomers bind tightly to the PAA polyelectrolyte. The dynamics of the AN monomers are more likely to behave as part of the polymer which results in the shortening of relaxation time and thereby leads to the broadening of the proton peaks. As mentioned previously, AN is thought to be mainly protonated by CSA. It is likely that the AN/CSA complex interacts with PAA through H-bonding and that this interaction results in increased AN/CSA concentration along the PAA backbone. Therefore, we postulate that both acid−base and H-bonding interactions contribute to the stabilization of AN/CSA/PAA complex (Scheme 2).

Conclusion

Chiral PAA/PANI nanocomposites can be synthesized using a simplified template-guided synthesis procedure. High molecular weight PAA (MW 250 000) allows for the synthesis of dispersed chiral nanocomposites over a more broad concentration range. Stability of the PAA/AN/CSA adduct formed prior to polymerization influences the degree of PANI chirality. Adduct stability is influenced by reaction temperature and solvent content. The local concentration (aniline loading) and solution concentration (total concentration) prior to polymerization affect the degree of PANI chirality. We speculate that the rate of polymerization, competition of CSA with oxidant degradation products, and an increase in structural order with increasing AN/CSA concentration affect the degree of PANI chirality within PAA/PANI products. IR and NMR studies suggest that PANI and PAA are intimately mixed at the molecular level. All of the results are consistent with our proposed mechanism and that complex formation between PAA, AN, and CSA is essential for the formation of chiral PAA/PANI.

Acknowledgment. H.L.W. thanks for financial support the Laboratory Directed Research and Development (LDRD) fund from Los Alamos National Laboratory (DOE) and the Cross Enterprise Technology Development Program from National Aeronautics and Space Administration (NASA).

References and Notes

(1) Kanatzidis, M. G.; Wu, C. G.; Marcy, H. O.; Degroot, D. C.; Kannewurf, C. R. *Chem. Mater.* **1990**, *2*, 222−224.
(2) Aldissi, M.; Armes, S. P. *Prog. Org. Coat.* **1991**, *19*, 21−58.
(3) Armes, S. P.; Aldissi, M.; Hawley, M.; Beery, J. G.; Gottesfeld, S. *Langmuir* **1991**, *7*, 1447−1452.
(4) Stejskal, J.; Kratochvil, P.; Gospodinova, N.; Terlemezyan, L.; Mokreva, P. *Polymer* **1992**, *33*, 4857−4858.
(5) Stejskal, J.; Kratochvil, P.; Radhakrishnan, N. *Synth. Met.* **1993**, *61*, 225−231.
(6) Stejskal, J.; Kratochvil, P.; Gospodinova, N.; Terlemezyan, L.; Mokreva, P. *Polym. Int.* **1993**, *32*, 401−405.
(7) Liu, J. M.; Yang, S. C. *J. Chem. Soc., Chem. Commun.* **1991**, 1529−1531.
(8) Armes, S. P.; Aldissi, M.; Agnew, S.; Gottesfeld, S. *Langmuir* **1990**, *6*, 1745−1749.
(9) Banerjee, P.; Bhattacharyya, S. N.; Mandal, B. M. *Langmuir* **1995**, *11*, 2414−2418.
(10) Yoneyama, H.; Kuwabata, S. *Denki Kagaku* **1997**, *65*, 814−819.
(11) Yoneyama, H.; Ii, Y.; Kuwabata, S. *J. Electrochem. Soc.* **1992**, *139*, 28−32.
(12) Kryszewski, M.; Jeszka, J. K. *Synth. Met.* **1998**, *94*, 99−104.
(13) Esteban, P. O.; Leger, J. M.; Lamy, C.; Genies, E. *J. Appl. Electrochem.* **1989**, *19*, 462−464.
(14) Innis, P. C.; Norris, I. D.; KaneMaguire, L. A. P.; Wallace, G. G. *Macromolecules* **1998**, *31*, 6521−6528.
(15) Aboutanos, V.; Barisci, J. N.; KaneMaguire, L. A. P.; Wallace, G. G. *Synth. Met.* **1999**, *106*, 89−95.
(16) McCarthy, P. A.; Huang, J. Y.; Yang, S. C.; Wang, H. L. *Langmuir* **2002**, *18*, 259−263.
(17) RaultBerthelot, J.; Raoult, E.; TahriHassani, J.; LeDeit, H.; Simonet, J. *Electrochim. Acta* **1999**, *44*, 3409−3419.
(18) Moutet, J. C.; Saintaman, E.; Tranvan, F.; Angibeaud, P.; Utille, J. P. *Adv. Mater.* **1992**, *4*, 511−513.
(19) Guo, H. L.; Knobler, C. M.; Kaner, R. B. *Synth. Met.* **1999**, *101*, 44−47.
(20) Eisazadeh, H.; Spinks, G.; Wallace, G. G. *Polymer* **1994**, *35*, 3801−3803.
(21) Majidi, M. R.; Kanemaguire, L. A. P.; Wallace, G. G. *Polymer* **1995**, *36*, 3597−3599.
(22) Majidi, M. R.; KaneMaguire, L. A. P.; Wallace, G. G. G. *Polymer* **1996**, *37*, 359−362.
(23) Zhou, Y. X.; Yu, B.; Zhu, G. Y. *Polymer* **1997**, *38*, 5493−5495.
(24) Akagi, K.; Piao, G.; Kaneko, S.; Sakamaki, K.; Shirakawa, H.; Kyotani, M. *Science* **1998**, *282*, 1683−1686.
(25) LangeveldVoss, B. M. W.; Peeters, E.; Janssen, R. A. J.; Meijer, E. W. *Synth. Met.* **1997**, *84*, 611−614.
(26) Ashraf, S. A.; KaneMaguire, L. A. P.; Majidi, M. R.; Pyne, S. G.; Wallace, G. G. *Polymer* **1997**, *38*, 2627−2631.
(27) Yashima, E.; Maeda, K.; Okamoto, Y. *Nature (London)* **1999**, *399*, 449−451.
(28) McCarthy, P. A.; Huang, J.; Yang, S.-C.; Wang, H.-L. *Langmuir* **2002**, *18*, 259.

(29) Mattoso, L. H. C.; Macdiarmid, A. G.; Epstein, A. J. *Synth. Met.* **1994**, *68*, 1−11.
(30) Adams, P. N.; Laughlin, P. J.; Monkman, A. P.; Kenwright, A. M. *Polymer* **1996**, *37*, 3411−3417.
(31) MacDiarmid, A. G. *Synth. Met.* **1997**, *84*, 27−34.
(32) Fiesel, R.; Huber, J.; Apel, U.; Enkelmann, V.; Hentschke, R.; Scherf, U.; Cabrera, K. *Macromol. Chem. Phys.* **1997**, *198*, 2623−2650.
(33) Mohney, B. K.; Petri, E. T.; Uvarova, V.; Walker, G. C. *Appl. Spectrosc.* **2000**, *54*, 9−14.
(34) Dong, J.; Ozaki, Y.; Nakashima, K. *Macromolecules* **1997**, *30*, 1111−1117.
(35) Dong, J.; Ozaki, Y.; Nakashima, K. *J. Polym. Sci., Part B: Polym. Phys.* **1997**, *35*, 507−515.
(36) Ilic, M.; Koglin, E.; Pohlmeier, A.; Narres, H. D.; Schwuger, M. J. *Langmuir* **2000**, *16*, 8946−8951.
(37) Trchova, M.; Stejskal, J.; Prokes, J. *Synth. Met.* **1999**, *101*, 840−841.
(38) Liu, W.; Cholli, A. L.; Nagarajan, R.; Kumar, J.; Tripathy, S.; Bruno, F. F.; Samuelson, L. *J. Am. Chem. Soc.* **1999**, *121*, 11345−11355.

MA020915T